

# Fast Layout-Oblivious Tensor-Matrix Multiplication with BLAS

Cem Savaş Başsoy

Hamburg University of Technology, Schwarzenbergstrasse 95, Germany,  
cem.bassoy@gmail.com

**Abstract.** The tensor-matrix product is a basic tensor operation that is required by various tensor methods such as the ALS or the HOSVD. This paper presents flexible high-performance algorithms for the mode- $q$  tensor-matrix multiplication that computes the product according to the the Loops-over-gemms (LOG) approach with `gemm` being the general matrix multiply. Our algorithms can process dense tensors with any linear tensor layout, arbitrary tensor order and dimensions all of which can be runtime variable. We discuss different tensor slicing methods with parallelization strategies and propose six variations of a base algorithm which calls a `gemv`, `gemm` and/or a `gemm_batch` with subtensors or tensor slices. Their performance is quantified for a set of tensors with various shapes and tensor order. The best-performing version attains a median performance of 1.37 double precision Tflops/s on an Intel Xeon Gold 6248R processor using Intel’s MKL. We show that the performance is only slightly affected by the tensor layout and the median performance is between [?] and [?] Tflops/s for a range of linear tensor formats. Our fastest version of the tensor-matrix multiplication is on average at least 14.05% and up to 3.79 x faster than other state-of-the-art implementations, including Libtorch and Eigen.

## 1 Introduction

Tensor computations are found in many scientific fields such as computational neuroscience, pattern recognition, signal processing and data mining [7, 14]. Tensors representing large amount of multidimensional data are decomposed and analyzed with the help of basic tensor operations [8, 9]. The decomposition and analysis led to the development and analysis of high-performance kernels for tensor contractions. In this work, we present and analyze a high-performance algorithm for the tensor-matrix multiplication that is used in many numerical algorithms such as the alternating least squares method [8, 9]. It is a compute-bound tensor operation and has the same arithmetic intensity as a matrix-matrix multiplication which can almost reach the practical peak performance of a computing machine.

There has been three main approaches for implementing tensor contractions. The Transpose-Transpose-gemm-Transpose (TGGT) approach reorganizes (flattens) tensors in order to perform a tensor contraction with an optimized

matrix-matrix multiplication (`gemm`) implementation [2, 16]. Implementations of a more recent method (GETT) are based on high-performance `gemm`-like algorithms [1, 12, 17]. A different method is the LOG approach in which BLAS are utilized with multiple tensor slices or subtensors if possible [10, 13, 15]. Implementations of the LOG and TTGT approaches are in general easier to maintain and faster to port than GETT implementations which might need to adapt vector instructions or blocking parameters according to a processor’s micro-architecture.

Our work is motivated by the fact that LOG-based implementations of the tensor-matrix and tensor-vector multiplication are similar. To our best knowledge, we are the first to combine the approach in [3] with the findings in [10] and to propose fast in-place tensor-matrix multiplication algorithms that are layout-oblivious. Our algorithms compute the tensor-matrix product in parallel using OpenMP together with highly efficient `gemm` or `gemm_batch` implementations. They support dense tensors with any order, dimensions and any linear tensor layout including the first- and the last-order storage formats for any contraction mode all of which can be runtime variable. Input and output tensors do not need to be transposed or flattened into two-dimensional matrices. The parallel versions of the recursive base algorithm execute fused loops in parallel and are able to fully utilize a processors compute units. Despite, the generality of our approach, every proposed algorithm can be implemented with less than 100 lines of C++ code where the complexity is hidden by the BLAS implementation and the corresponding selection of subtensors or tensor slices. We have provided an open and free reference C++ implementation of all algorithms and a python interface for convenience. While we have used Intel’s MKL for our benchmarks, the user is free to choose any other library that provides the BLAS interface.

The following analysis quantifies the impact of the tensor layout, the tensor slicing method and parallel execution of slice-matrix multiplications with varying contraction modes. The runtime measurements of our implementations are compared with those presented in [12, 17] including Libtorch and Eigen. In summary, the main findings of our work are:

- A tensor-matrix multiplication can be implemented by an in-place algorithm with 1 `gemv` and 7 `gemm` calls supporting all combinations of contraction mode, tensor order and dimensions for any linear tensor layout.
- Our algorithm with variable loop fusion and parallel slice-matrix multiplications is on average 17% faster than a single batched `gemm` call when the contraction and leading dimensions are greater than 256.
- All our proposed algorithms are layout oblivious and achieve at least a median throughput of [?] for any linear tensor layout.
- Our LOG-based tensor-times-matrix implementation are in general faster than TTGT- and GETT-based implementations that have been described in [12, 17] including actively developed libraries such as Libtorch and Eigen. Using symmetrically shaped tensors, an average speedup of [?] x to [?] x for single and double precision floating point computations can be achieved.

The remainder of the paper is organized as follows. Section 2 presents related work. Section 3 introduces the terminology used in this paper and defines the

85 tensor-vector multiplication. Algorithm design and methods for parallel execu-  
 86 tion is discussed in Section 4. Section 5 describes the test setup and discusses  
 87 the benchmark results in Section 6. Conclusions are drawn in Section 7.

## 88 2 Related Work

89 The authors in [13] discuss the efficient tensor contractions with highly optimized  
 90 BLAS. Based on the LOG approach, they define requirements for the use of GEMM for  
 91 class 3 tensor contractions and provide slicing techniques for tensors. The slicing  
 92 recipe for the class 2 categorized tensor contractions contains a short description  
 93 with a rule of thumb for maximizing performance. Runtime measurements cover  
 94 class 3 tensor contractions.

95 The work in [10] presents a framework that generates in-place tensor-matrix  
 96 multiplication according to the LOG approach. The authors present two strategies  
 97 for efficiently computing the tensor contraction applying GEMMs with tensors.  
 98 They report a speedup of up to 4x over the TTGT-based MATLAB tensor toolbox  
 99 library discussed in [2]. Although many aspects are similar to our work, the  
 100 authors emphasize the code generation of tensor-matrix multiplications using  
 101 high-performance GEMM's.

102 The authors of [17] present a tensor-contraction generator TCCG and the GETT  
 103 approach for dense tensor contractions that is inspired from the design of a high-  
 104 performance GEMM. Their unified code generator selects implementations from  
 105 generated GETT, LoG and TTGT candidates. Their findings show that among 48 dif-  
 106 ferent contractions 15% of LoG based implementations are the fastest. However,  
 107 their tests do not include the tensor-vector multiplication where the contraction  
 108 exhibits at least one free tensor index.

109 Using also the GETT approach, the author presents in [12] a runtime flexible  
 110 tensor contraction library. He describes block-scatter-matrix algorithm which  
 111 uses a special layout for the tensor contraction. The proposed algorithm yields  
 112 results that feature a similar runtime behavior to those presented in [17].

## 113 3 Background

114 **Notation** An order- $p$  tensor is a  $p$ -dimensional array [11] where tensor ele-  
 115 ments are contiguously stored in memory. We write  $a$ ,  $\mathbf{a}$ ,  $\mathbf{A}$  and  $\underline{\mathbf{A}}$  in order to  
 116 denote scalars, vectors, matrices and tensors. If not otherwise mentioned, we  
 117 assume  $\underline{\mathbf{A}}$  to have a tensor order that is greater than 2. The  $p$ -tuple  $\mathbf{n}$  with  
 118  $\mathbf{n} = (n_1, n_2, \dots, n_p)$  will be referred to as a dimension tuple with  $n_r > 1$ . We  
 119 will use round brackets  $\underline{\mathbf{A}}(i_1, i_2, \dots, i_p)$  or  $\underline{\mathbf{A}}(\mathbf{i})$  to denote a tensor element where  
 120  $\mathbf{i} = (i_1, i_2, \dots, i_p)$  is a multi-index. A subtensor is denoted by  $\underline{\mathbf{A}}'$  and references  
 121 elements of a tensor  $\underline{\mathbf{A}}$ . They are specified with  $p$  index ranges and form a selec-  
 122 tion grid. In this work, the index range shall either address all indices of a given  
 123 mode or a single element that are given by single indices  $i_r$  with  $1 \leq r \leq p$ .  
 124 Elements  $n'_r$  of a subtensor's dimension tuple  $\mathbf{n}'$  are therefore  $n_r$  if all indices  
 125 of mode  $r$  are selected and 1 otherwise. We will annotate subtensors using only

their non-unit modes such as  $\underline{\mathbf{A}}'_{u,v,w}$  where  $n_u > 1, n_v > 1$  and  $n_w > 1$  and  $1 \leq u \neq v \neq w \leq p$ . It is sufficient to only provide non-unit modes as the remaining single indices correspond to the loop induction variables of the following algorithms. A subtensor is called a slice  $\underline{\mathbf{A}}'_{u,v}$  if the full range selection of  $\underline{\mathbf{A}}$  occurs with only two modes. A fiber  $\underline{\mathbf{A}}'_u$  is a tensor slice with only one dimension greater than 1.

**Linear Tensor Layouts** We use a layout tuple  $\boldsymbol{\pi} \in \mathbb{N}^p$  to encode all linear tensor layouts including the first-order or last-order layout. They contain permuted tensor modes whose priority is given by their index. For instance, the first- and last-order storage formats are given by  $\boldsymbol{\pi}_F = (1, 2, \dots, p)$  and  $\boldsymbol{\pi}_L = (p, p-1, \dots, 1)$ . An inverse layout tuple  $\boldsymbol{\pi}^{-1}$  is defined by  $\boldsymbol{\pi}^{-1}(\boldsymbol{\pi}(k)) = k$ . Given a layout tuple  $\boldsymbol{\pi}$  with  $p$  modes, the  $\pi_r$ -th element of a stride tuple is given by  $w_{\pi_r} = \prod_{k=1}^{r-1} n_{\pi_k}$  for  $1 < r \leq p$  and  $w_{\pi_1} = 1$ . Tensor elements of the  $\pi_1$ -th mode are contiguously stored in memory.

The location of tensor elements is determined by the tensor layout and the layout function. For a given tensor layout and stride tuple, a layout function  $\lambda_{\mathbf{w}}$  maps a multi-index to a scalar index with  $\lambda_{\mathbf{w}}(\mathbf{i}) = \sum_{r=1}^p w_r(i_r - 1)$ . With  $j = \lambda_{\mathbf{w}}(\mathbf{i})$  being the relative memory position of an element with a multi-index  $\mathbf{i}$ , reading from and writing to memory is accomplished with  $j$  and the first element's address of  $\underline{\mathbf{A}}$ .

**Non-Modifying Flattening and Reshaping** The flattening operation  $\varphi_{r,q}$  transforms an order- $p$  tensor  $\underline{\mathbf{A}}$  to another order- $p'$  view  $\underline{\mathbf{B}}$  that has different a shape  $\mathbf{m}$  and layout  $\boldsymbol{\tau}$  tuple of length  $p'$  with  $p' = p - q + r$  and  $1 \leq r < q \leq p$ . It is related to the tensor unfolding operation as defined in [8, p.459] but neither changes the element ordering nor copies tensor elements. Given a layout tuple  $\boldsymbol{\pi}$  of  $\underline{\mathbf{A}}$ , the flattening operation  $\varphi_{r,q}$  is defined for contiguous modes  $\hat{\boldsymbol{\pi}} = (\pi_r, \pi_{r+1}, \dots, \pi_q)$  of  $\boldsymbol{\pi}$ . Let  $j = 0$  if  $k \leq r$  and  $j = q - r$  otherwise for  $1 \leq k \leq p'$ . Then the resulting layout tuple  $\boldsymbol{\tau} = (\tau_1, \dots, \tau_{p'})$  of  $\underline{\mathbf{B}}$  is given by  $\tau_r = \min(\boldsymbol{\pi}_{r,q})$  and  $\tau_k = \pi_{k+j} + s_k$  if  $k \neq r$  where  $s_k = |\{\pi_i \mid \pi_{k+j} > \pi_i \wedge \pi_i \neq \min(\hat{\boldsymbol{\pi}}) \wedge r \leq i \leq p\}|$ . Elements of the corresponding shape tuple  $\mathbf{m}$  are given by  $m_{\tau_r} = \prod_{k=r}^q n_{\pi_k}$  and  $m_{\tau_k} = n_{\pi_{k+j}}$  if  $k \neq r$ .

The reshaping operation  $\rho$  transforms an order- $p$  tensor  $\underline{\mathbf{A}}$  to another order- $p$  tensor  $\underline{\mathbf{B}}$  with different shape  $\mathbf{m}$  and layout  $\boldsymbol{\tau}$  tuples of length  $p$ . In this work, it permutes the shape and layout tuple simultaneously without changing the element ordering and without copying tensor elements. The operation  $\rho$  uses a permutation tuple  $\boldsymbol{\rho} = (\rho_1, \dots, \rho_p)$  to only modify shape and layout tuples. Elements of the resulting shape tuple  $\mathbf{m}$  and the layout tuple  $\boldsymbol{\tau}$  are given by  $m_r = n_{\rho_r}$  and  $\tau_r = \pi_{\rho_r}$ , respectively.

**Tensor-Matrix Multiplication (TTM)** Let  $\underline{\mathbf{A}}$  and  $\underline{\mathbf{C}}$  be order- $p$  tensors with shapes  $\mathbf{n}_a = (n_1, \dots, n_q, \dots, n_p)$  and  $\mathbf{n}_c = (n_1, \dots, n_{q-1}, m, n_{q+1}, \dots, n_p)$ . Let  $\underline{\mathbf{B}}$  be a matrix of shape  $\mathbf{n}_b = (m, n_q)$ . A mode- $q$  TTM is denoted by  $\underline{\mathbf{C}} = \underline{\mathbf{A}} \times_q \underline{\mathbf{B}}$

167 where an element of  $\underline{\mathbf{C}}$  is given by

$$\underline{\mathbf{C}}(i_1, \dots, i_{q-1}, j, i_{q+1}, \dots, i_p) = \sum_{i_q=1}^{n_q} \underline{\mathbf{A}}(i_1, \dots, i_q, \dots, i_p) \cdot \mathbf{B}(j, i_q) \quad (1)$$

168 with  $1 \leq i_r \leq n_r$  and  $1 \leq j \leq m$ . The mode  $q$  is the *contraction mode* of  
 169 the TTM with  $1 \leq q \leq p$ . The tensor-matrix multiplication generalizes the  
 170 computational aspect of the two-dimensional case  $\mathbf{C} = \mathbf{B} \cdot \mathbf{A}$  if  $p = 2$  and  $q = 1$ .  
 171 Its arithmetic intensity is equal to that of a matrix-matrix multiplication and  
 172 is not memory-bound. In the following, we assume that the tensors  $\underline{\mathbf{A}}$  and  $\underline{\mathbf{C}}$   
 173 have the same tensor layout  $\boldsymbol{\pi}$ . Elements of matrix  $\mathbf{B}$  can stored in either the  
 174 column-major or row-major format.

## 175 4 Algorithm Design

### 176 4.1 Sequential Algorithm

177 The sequential baseline algorithm for Eq. 1 can be implemented with a single  
 178 C++ function that supports tensors with arbitrary order, dimensions and any  
 179 linear tensor layout. It consists of nested recursion with a control flow that is akin  
 180 to algorithm 1 in [4] consisting of two **if** statements with an **else** branch. The  
 181 body of the first **if** statement contains a recursive call that skips the iteration  
 182 over the dimension  $n_q$  when  $r = \hat{q}$  with  $\pi_r = q$  and  $\hat{q} = \boldsymbol{\pi}_q^{-1}$  where  $\boldsymbol{\pi}^{-1}$  is the  
 183 inverse layout tuple. The second **if** statement contains multiple recursive calls  
 184 for the modes  $1 \leq r \neq \hat{q} \leq p$  with different multi-indices. The **else** branch is the  
 185 base case and consists of two loops that compute a fiber-matrix product. The  
 186 outer loop iterates with  $j$  over the dimension  $m$  of  $\underline{\mathbf{C}}$  and  $\mathbf{B}$ . The inner loop  
 187 iterates with  $i_q$  over the dimension  $n_q$  of  $\underline{\mathbf{A}}$  and  $\mathbf{B}$  computing an inner product.

### 188 4.2 Baseline Algorithm with Contiguous Memory Access

189 The baseline algorithm accesses elements of  $\underline{\mathbf{A}}$  and  $\underline{\mathbf{C}}$  non-contiguously whenever  
 190  $\pi_1 \neq q$ . Matrix  $\mathbf{B}$  is contiguously accessed if  $i_q$  or  $j$  is incremented with unit-  
 191 steps depending on the storage format of  $\mathbf{B}$ . The access pattern can be improved  
 192 by reordering tensor elements according to the storage format. However, copy  
 193 operations reduce the overall throughput of the operation [15].

194 A better approach is to access tensor elements according to the tensor layout  
 195 using the tensor layout tuple  $\boldsymbol{\pi}$  as proposed in [4]. The modified algorithm 1  
 196 contiguously accesses memory for  $\pi_1 \neq q$  and  $p > 1$ . Each recursion level adjusts  
 197 only one multi-index element  $i_{\pi_r}$  with a stride  $w_{\pi_r}$  in line 5. With increasing re-  
 198 cursion level and decreasing  $r$ , indices are incremented with smaller step sizes as  
 199  $w_{\pi_r} \leq w_{\pi_{r+1}}$ . The condition of the second **if** statement in line 4 is changed from  
 200  $r \geq 1$  to  $r > 1$ . In this way, the mode- $\pi_1$  loop with index  $i_{\pi_1}$  and the minimum  
 201 stride  $w_{\pi_1}$  are included in the base case which contains three loops performing  
 202 a slice-matrix multiplication. The loop ordering are adjusted according to the

---

```

1 tensor_times_matrix(A, B, C, n, i, m, q, q̂, r)
2   if  $r = \hat{q}$  then
3     | tensor_times_matrix(A, B, C, n, i, m, q, q̂,  $r - 1$ )
4   else if  $r > 1$  then
5     | for  $i_{\pi_r} \leftarrow 1$  to  $n_{\pi_r}$  do
6       | | tensor_times_matrix(A, B, C, n, i, m, q, q̂,  $r - 1$ )
7   else
8     | for  $j \leftarrow 1$  to  $m$  do
9       | | for  $i_q \leftarrow 1$  to  $n_q$  do
10        | | | for  $i_{\pi_1} \leftarrow 1$  to  $n_{\pi_1}$  do
11          | | | | C( $i_1, \dots, i_{q-1}, j, i_{q+1}, \dots, i_p$ ) += A( $i_1, \dots, i_q, \dots, i_p$ ) · B( $j, i_q$ )

```

---

**Algorithm 1:** Modified baseline algorithm with contiguous memory access for the tensor-matrix multiplication. The tensor order must be greater than one and for the contraction mode  $1 \leq q \leq p$  and  $\pi_1 \neq q$  must hold. The algorithm needs to be initially called with  $r = p$  where  $\mathbf{n}$  is the shape tuple of  $\underline{\mathbf{A}}$  and  $m$  is the  $q$ -th dimension of  $\underline{\mathbf{C}}$ .

203 tensor and matrix layout. The inner-most loop increments  $i_{\pi_1}$  and contiguously  
 204 accesses tensor elements of  $\underline{\mathbf{A}}$  and  $\underline{\mathbf{C}}$ . The second loop increments  $i_q$  with which  
 205 elements of  $\mathbf{B}$  are contiguously accessed if  $\mathbf{B}$  is stored in the row-major format.  
 206 The third loop increments  $j$  and could be placed as the second loop if  $\mathbf{B}$  is stored  
 207 in the column-major format.

208 While spatial data locality is improved by adjusting the loop ordering, the  
 209 temporal data locality of tensors  $\underline{\mathbf{A}}$  and  $\underline{\mathbf{C}}$  differ. Note that slice  $\underline{\mathbf{A}}'_{\pi_1, q}$  is accessed  
 210  $m$  times, fiber  $\underline{\mathbf{C}}_{\pi_1}$  is accessed  $\mathbf{n}(q)$  times and element  $\underline{\mathbf{B}}(j, i_q)$  is accessed  $\mathbf{n}(\pi_1)$   
 211 times. While the specified fiber of  $\underline{\mathbf{C}}$  can fit into first or second level cache, slice  
 212 elements of  $\underline{\mathbf{A}}$  are unlikely to fit in the local caches if the slice size  $n_{\pi_1} \times n_q$   
 213 is large leading to higher cache misses and suboptimal performance. Optimized  
 214 tiling for better temporal data locality has been discussed in [6] which suggests  
 215 to use existing high-performance BLAS implementations for the base case.

### 216 4.3 BLAS-based Algorithms with Tensor Slices

217 Algorithm 1 is the starting point for the BLAS-based algorithm which computes  
 218 the tensor-matrix product with a `gemm` routine. Besides the illustrated algorithm,  
 219 we have identified seven other cases where a single `gemm` call suffices to compute  
 220 the tensor-matrix product even if the tensor order  $p > 2$ . In summary, there  
 221 are eight cases with a single `gemm` call using different arguments which are listed  
 222 in table 1. The list of `gemm` calls supports all linear tensor layout and has no  
 223 limitation on tensor order and contraction mode. The arguments of `gemm` are  
 224 chosen depending on the tensor order  $p$ , tensor layout  $\boldsymbol{\pi}$  and contraction mode  
 225  $q$  except for the `CBLAS_ORDER` which is `CblasRowMajor`.

Case	Order $p$	Layout $\pi$	Mode $q$	Routine	T	M	N	K	A	LDA	B	LDB	LDC
1	1	-	1	<b>gemv</b>	-	$m$	$n_1$	-	<b>B</b>	$n_1$	<u><b>A</b></u>	-	-
2	2	(1, 2)	1	<b>gemm</b>	<b>B</b>	$n_2$	$m$	$n_1$	<u><b>A</b></u>	$n_1$	<b>B</b>	$n_1$	$m$
3	2	(1, 2)	2	<b>gemm</b>	-	$m$	$n_1$	$n_2$	<b>B</b>	$n_2$	<u><b>A</b></u>	$n_1$	$n_1$
4	2	(2, 1)	1	<b>gemm</b>	-	$m$	$n_2$	$n_1$	<b>B</b>	$n_1$	<u><b>A</b></u>	$n_2$	$n_2$
5	2	(2, 1)	2	<b>gemm</b>	<b>B</b>	$n_1$	$m$	$n_2$	<u><b>A</b></u>	$n_2$	<b>B</b>	$n_2$	$m$
6	$> 2$	any	$\pi_1$	<b>gemm</b>	<b>B</b>	$\bar{n}_q$	$m$	$n_q$	<u><b>A</b></u>	$n_q$	<b>B</b>	$n_q$	$m$
7	$> 2$	any	$\pi_p$	<b>gemm</b>	-	$m$	$\bar{n}_q$	$n_q$	<b>B</b>	$n_q$	<u><b>A</b></u>	$\bar{n}_q$	$\bar{n}_q$
8	$> 2$	any	$\pi_2, \dots, \pi_{p-1}$	<b>gemm*</b>	-	$m$	$n_{\pi_1}$	$n_q$	<b>B</b>	$n_q$	<u><b>A</b></u>	$w_q$	$w_q$

**Table 1.** Eight **gemv** and **gemm** cases for the mode- $q$  tensor-matrix multiplication. Arguments T, M, N, etc. of the BLAS are chosen with respect to the tensor order  $p$ , layout  $\pi$  and contraction mode  $q$  where T specifies if **B** is transposed. **gemm\*** denotes multiple **gemm** calls with different tensor slices. Argument  $\bar{n}_q$  for case 6 and 7 is given by  $\bar{n}_q = 1/n_q \prod_r n_r$ . Matrix **B** has the row-major format.

226 *Case 1* ( $p = 1$ ): The tensor-vector product  $\underline{\mathbf{A}} \times_1 \mathbf{B}$  can be computed with a  
 227 **gemv** operation  $\mathbf{a}^T \cdot \mathbf{B}$  where **A** is an order-1 tensor, i.e. a vector **a** of length  $n_1$ .

228 *Case 2-5* ( $p = 2$ ): If **A** and **C** are order-2 tensors, i.e. a matrix **A** with  
 229 dimensions  $n_1$  and  $n_2$ , then a single **gemm** suffices to compute the tensor-matrix  
 230 product. If **A** and **C** have the column-major format with  $\pi = (1, 2)$ , **gemm** either  
 231 executes  $\mathbf{C} = \mathbf{A} \cdot \mathbf{B}^T$  for  $q = 1$  or  $\mathbf{C} = \mathbf{B} \cdot \mathbf{A}$  for  $q = 2$ . Note that **gemm** interprets  
 232 **C** and **A** as matrices using the reshaping operation  $\rho$  with  $\rho = (2, 1)$  in row-  
 233 major format even though both are stored column-wise. If **A** and **C** have the  
 234 row-major format with  $\pi = (2, 1)$ , **gemm** either executes  $\mathbf{C} = \mathbf{B} \cdot \mathbf{A}$  for  $q = 1$  or  
 235  $\mathbf{C} = \mathbf{A} \cdot \mathbf{B}^T$  for  $q = 2$ . Note that the transposition of **B** is necessary for the cases  
 236 2,5 and independent of the chosen storage format.

237 *Case 6-7* ( $p > 2$ ): If the order of **A** and **C** is greater than 2 and if the  
 238 contraction mode  $q$  is equal to  $\pi_1$  (case 6), a single **gemm** with the depicted  
 239 parameters executes  $\mathbf{C} = \mathbf{A} \cdot \mathbf{B}^T$  and computes a tensor-matrix product  $\underline{\mathbf{C}} =$   
 240  $\underline{\mathbf{A}} \times_{\pi_1} \mathbf{B}$  for any storage layout of **A** and **C**. Tensors **A** and **C** are flattened with  
 241  $\varphi_{2,p}$  to row-major matrices **A** and **C**. Matrix **A** has  $\bar{n}_{\pi_1} = \bar{n}/n_{\pi_1}$  rows and  $n_{\pi_1}$   
 242 columns while matrix **C** has the same number of rows and  $m$  columns. If  $\pi_p = q$   
 243 (case 7), Tensors **A** and **C** are flattened with  $\varphi_{1,p-1}$  to column-major matrices  
 244 **A** and **C**. Matrix **A** has  $n_{\pi_p}$  rows and  $\bar{n}_{\pi_p} = \bar{n}/n_{\pi_p}$  columns while matrix **C**  
 245 has  $m$  rows and the same number of columns. A single **gemm** executes  $\mathbf{C} = \mathbf{B} \cdot \mathbf{A}$   
 246 and computes the tensor-matrix product  $\underline{\mathbf{C}} = \underline{\mathbf{A}} \times_{\pi_p} \mathbf{B}$  for any storage layout  
 247 of **A** and **C**. Note that in all cases no copy operation is performed in order to  
 248 compute the desired contraction, see subsection 3.

249 *Case 8* ( $p > 2$ ): If the tensor order is greater than 2 with  $\pi_1 \neq q$  and  $\pi_p \neq q$ ,  
 250 the modified baseline algorithm 1 is used to successively call  $\bar{n}/(n_q \cdot n_{\pi_1})$  times  
 251 **gemm** with different tensor slices of **C** and **A** in the base case. Each **gemm** computes  
 252 one slice  $\underline{\mathbf{C}}'_{\pi_1,q}$  of the tensor-matrix product  $\underline{\mathbf{C}}$  using the corresponding tensor  
 253 slices **A**' $_{\pi_1,q}$  and the matrix **B**. The matrix-matrix product  $\mathbf{C} = \mathbf{B} \cdot \mathbf{A}$  is performed

by interpreting both tensor slices as row-major matrices  $\mathbf{A}$  and  $\mathbf{C}$  which have the dimensions  $(n_q, n_{\pi_1})$  and  $(m, n_{\pi_1})$ , respectively.

#### 4.4 BLAS-Based Algorithms with Subtensors

Case 8 can be optimized by selecting larger subtensors instead of tensor slices which might lead to a better processor utilization. Larger subtensors can be used by selecting additional mergeable modes that still allow the subtensor to be flattened into a matrix without reordering tensor elements using the description provided in section 3, see also lemma 4.1 in [10]. The maximum number of mergeable modes is  $\hat{q} - 1$  with  $\hat{q} = \pi^{-1}(q)$  and the corresponding modes are  $\pi_1, \pi_2, \dots, \pi_{\hat{q}-1}$ . Applying flattening  $\varphi_{1,q-1}$  and reshaping  $\rho$  with  $\boldsymbol{\rho} = (2, 1)$  on a subtensor of  $\underline{\mathbf{A}}$  with dimensions  $n_{\pi_1}, \dots, n_{\pi_{\hat{q}-1}}, n_q$  yields a row-major matrix  $\mathbf{A}$  with shape  $(n_q, \prod_{r=1}^{\hat{q}-1} n_{\pi_r})$ . This is done analogously for  $\underline{\mathbf{C}}$  resulting in a row-major matrix with shape  $(m, \prod_{r=1}^{\hat{q}-1} n_{\pi_r})$ . This description supports all linear tensor layouts and generalizes lemma 4.2 in [10].

Algorithm 1 needs a minor modification for calling `gemm` flattened subtensors instead of tensor slices. The modified algorithm must therefore omit the first  $\hat{q}$  modes  $\boldsymbol{\pi}_{1,\hat{q}} = (\pi_1, \dots, \pi_{\hat{q}})$  including  $\pi_{\hat{q}} = q$ . This is done by only iterating over modes larger than  $\hat{q}$  in the non-base case. The conditions in line 2 and 4 are changed to  $1 < r \leq \hat{q}$  and  $\hat{q} < r$ , respectively. The single indices of the subtensors  $\underline{\mathbf{A}}'_{\boldsymbol{\pi}_{1,\hat{q}}}$  and  $\underline{\mathbf{C}}'_{\boldsymbol{\pi}_{1,\hat{q}}}$  are given by the loop induction variables that belong to the  $\pi_r$ -th loop with  $\hat{q} + 1 \leq r \leq p$ .

#### 4.5 Parallel BLAS-based Algorithms

The following paragraphs discuss three parallel approaches for the eighth case. Cases 1 to 7 already call a multi-threaded `gemm` and cannot be further optimized.

**Sequential Loops and Multithreaded `gemm`** One straight forward approach is to use algorithm 1 as it is and to sequentially call a multi-threaded `gemm` in the base case of the algorithm as described in subsection 4.4. This is beneficial if  $q = \pi_{p-1}$ , the inner dimensions  $n_{\pi_1}, \dots, n_q$  are large or the outer-most dimension  $n_{\pi_p}$  is smaller than the available processor cores. However, if the above conditions are not met, the processor cores might not be fully utilized where each multi-threaded `gemm` is executed with small subtensors. We will refer to this algorithm version as `<seq-loops,par-gemm>` that is executable with subtensors or tensor slices.

**Parallel Loops and Single- or Multithreaded `gemm`** A more advanced version of the above algorithm executes a single-threaded `gemm` in parallel including all available (free) modes which depend on the slicing. If subtensors are used, all  $\pi_{\hat{q}+1}, \dots, \pi_p$  modes are free. In case of tensor slices, only  $\pi_1$  and  $\pi_{\hat{q}}$  are free modes. The corresponding maximum degree of parallelism for both cases are  $\prod_{r=\hat{q}+1}^p n_{\pi_r}$  and  $\prod_{r=1}^p n_r / (n_{\pi_1} n_{\pi_{\hat{q}}})$ , respectively.



Using tensor slices for the multiplication,  $\underline{\mathbf{A}}$  and  $\underline{\mathbf{C}}$  are flattened twice with  $\varphi_{\pi_{\hat{q}+1}, \pi_p}$  and  $\varphi_{\pi_2, \pi_{\hat{q}-1}}$ . The resulting tensor is of order 4 with dimensions  $n_{\pi_1}, \hat{n}_{\pi_2}, n_q, \hat{n}_{\pi_4}$  where  $\hat{n}_{\pi_2} = \prod_{r=2}^{\hat{q}-1} n_{\pi_r}$  and  $\hat{n}_{\pi_4} = \prod_{r=\hat{q}+1}^p n_{\pi_r}$ . In this way the tree-recursion has been transformed in two loops. The outer loop iterates over  $\hat{n}_{\pi_4}$  while the inner loop iterates over  $\hat{n}_{\pi_2}$  calling `gemm` with slices  $\underline{\mathbf{A}}'_{\pi_1, q}$  and  $\underline{\mathbf{C}}'_{\pi_1, q}$ . Both loops are parallelized using `omp parallel for` together with the `collapse(2)` and the `num_threads` clause which specifies the thread number.

In case of the general subtensor-matrix approach, both tensors are flattened twice with  $\varphi_{\pi_{\hat{q}+1}, \pi_p}$  and  $\varphi_{\pi_1, \pi_{\hat{q}-1}}$ . The resulting tensor is of order 3 with dimensions  $\hat{n}_{\pi_1}, n_q, \hat{n}_{\pi_4}$  where  $\hat{n}_{\pi_1} = \prod_{r=1}^{\hat{q}-1} n_{\pi_r}$  and  $\hat{n}_{\pi_4} = \prod_{r=\hat{q}+1}^p n_{\pi_r}$ . The corresponding algorithm consists of one loops which iterates over  $\hat{n}_{\pi_4}$  calling single-threaded `gemm` with multiple subtensors  $\underline{\mathbf{A}}'_{\pi', q}$  and  $\underline{\mathbf{C}}'_{\pi', q}$  with  $\pi' = (\pi_1, \dots, \pi_{\hat{q}-1})$ .

Both algorithm variants will be referred to as `<par-loops, seq-gemm>` which can be used with subtensors or tensor slices. Note that `<seq-loops, par-gemm>` and `<par-loops, seq-gemm>` are opposing versions where either `gemm` or the free loops are performed in parallel. The all-parallel version `<par-loops, par-gemm>` executes available loops in parallel where each loop thread executes a multi-threaded `gemm` with either subtensors or tensor slices.

**Multithreaded `gemm_batch`** The next version of the base algorithm is a modified version of the general subtensor-matrix approach that calls a single batched `gemm` for the eighth case. The subtensor dimensions and remaining `gemm` arguments remain the same. The library implementation is responsible how subtensor-matrix multiplications are executed and if subtensors are further divided into smaller subtensors or tensor slices. This version will be referred to as the `<gemm_batch>` variant.

## 5 Experimental Setup

**Computing System** The experiments have been carried out on an Intel Xeon Gold 6248R processor with a Cascade micro-architecture. The processor consists of 24 cores operating at a base frequency of 3 GHz for non-AVX512 instructions. With 24 cores and a peak AVX-512 boost frequency of 2.5 GHz, the processor achieves a theoretical data throughput of ca. 1.92 double precision TFlops/s. We measured a peak performance of 1.78 double precision Tflops/s using the likwid performance tool.

The source code has been compiled with GCC v10.2 using the highest optimization level `-O3` and `-march=native`, `-pthread` and `-fopenmp`. Loops within for the eighth case have been parallelized using GCC's OpenMP v4.5 implementation. We have used the `GEMV` and `GEMM` implementation of the 2024.0 Intel MKL and its own threading library `mk1_intel_thread` together with the threading runtime library `libiomp5`.

If not otherwise mentioned, both tensors  $\underline{\mathbf{A}}$  and  $\underline{\mathbf{C}}$  are stored according to the first-order linear tensor layout with  $\pi = (1, \dots, p)$  whereas matrix  $\mathbf{B}$  has the row-major storage format. The benchmark results of each function are the average of 10 runs.

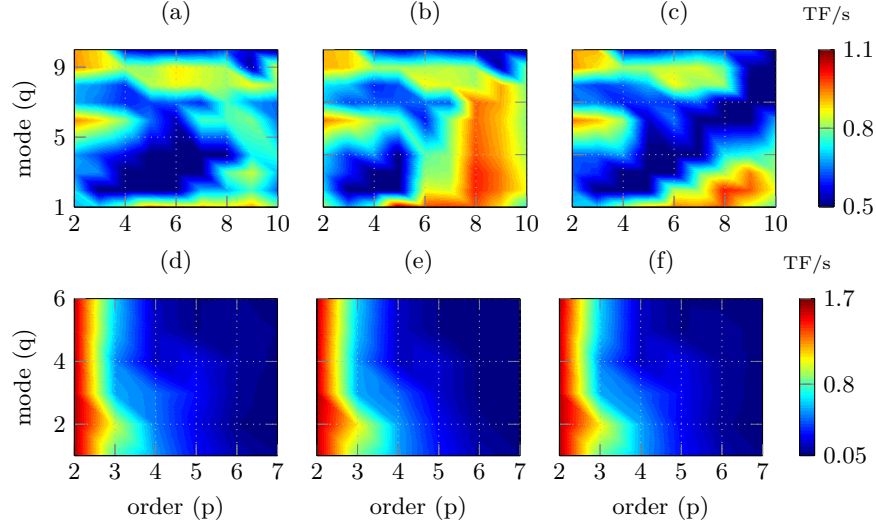


**Fig. 1.** Performance maps in double-precision Tflops/s of the proposed tensor-times-matrix algorithms with varying tensor orders  $p$  and contraction modes  $q$ . Tensors are asymmetrically-shaped on the upper plots and symmetrically-shaped on the lower plots. In (a) and (d) function `<gemm_batch>` is executed, in (b) and (e) `<par-loops, seq-gemm>` with tensor slices, in (c) and (f) `<par-loops, seq-gemm>` with subtensors.

**Tensor Shapes** We have used asymmetrically-shaped and symmetrically-shaped tensors in order to cover many possible use cases. The dimension tuples of both shape types are organized within two three-dimensional arrays with which tensors are initialized. The dimension array for the first shape type contains 720 =  $9 \times 8 \times 10$  dimension tuples where the row number is the tensor order ranging from 2 to 10. For each tensor order 8 tensor instances with increasing tensor size is generated. The second set consists of 336 =  $6 \times 8 \times 7$  dimensions tuples where the tensor order ranges from 2 to 7 and has 8 dimension tuples for each order. Each tensor dimension within the second set is  $2^{12}$ ,  $2^8$ ,  $2^6$ ,  $2^5$ ,  $2^4$  and  $2^3$ . A detailed explanation of the tensor shape setup is given in [3, 4].

## 6 Results and Discussion

**Slicing Methods** The following paragraphs analyze the two proposed slicing methods by benchmarking the functions `<par-loops, seq-gemm>` and `<gemm_batch>` using asymmetrically (top) and symmetrically (bottom) shaped tensors. Fig. 1 contains six contour plots (performance maps) in which `<par-loops, seq-gemm>` either uses subtensors or tensor slices and `<gemm_batch>` loops over subtensors only. Each point within the performance map represents a mean value that has been averaged over tensor sizes for a tensor order.

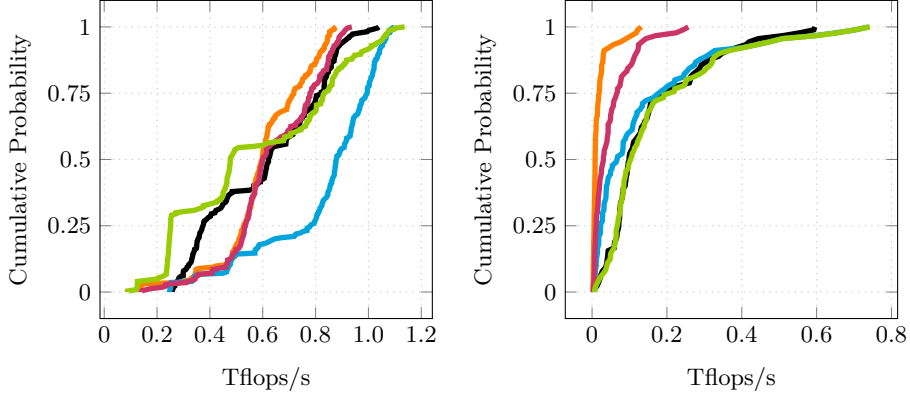


**Fig. 2.** Cumulative performance distributions of the proposed algorithms for case 8. Each distribution line belongs to one algorithm: `<gemm_batch>` (—), `<seq-loops,par-gemm>` (—) and `<par-loops,seq-gemm>` (—) using tensor slices, `<seq-loops,par-gemm>` (—) and `<par-loops,seq-gemm>` (—) using subtenors. Tensors are asymmetrically (left plot) and symmetrically shaped (right plot).

355 For asymmetrically shaped tensors, function `<par-loops,seq-gemm>` with ten-  
 356 sor slices performs on average 18% better than with subtenors. Surprisingly,  
 357 `<par-loops,seq-gemm>` with tensor slices is on average 11% faster than Intel’s  
 358 `gemm_batch` routine and reaches almost 1.1 Tflops/s for non-edge cases with  $q > 2$   
 359 and  $p > 6$ . This suggests that the Intel’s implementation might not divide sub-  
 360 tenors into smaller blocks.

361 With symmetrically shaped tensors, `<par-loops,seq-gemm>` with tensor slices  
 362 performs almost identical as `<gemm_batch>` with their respective median perfor-  
 363 mance of 221.52 Gflops/s and 236.21 Gflops/s. Moreover, the slicing method  
 364 almost has no affect on the runtime behavior of `<par-loops,seq-gemm>`. In con-  
 365 trast to the performance maps with asymmetrically shaped tensors, all functions  
 366 almost reach the attainable peak performance of 1.7 Tflops/s when  $p = 2$ . This  
 367 can be by the fact that both dimensions are equal or larger than 4096 enabling `gemm`  
 368 to operate under optimal conditions.

369 **Parallelization Methods** The nextz Applying the first setup configuration  
 370 with asymmetrically-shaped tensors, we have analyzed the effects of the blocking  
 371 and parallelization strategy. The LB-PN version processes tensors with different  
 372 storage formats, namely the 1-, 2-, 9- and 10-order layout. The performance  
 373 behavior is almost the same for all storage formats except for the corner cases  
 374  $q = \pi_1$  and  $q = \pi_p$ . Even the performance drop for  $q = p - 1$  is almost unchanged.  
 375 The standard deviation from the mean value is less than 10% for all storage  
 376 formats. Given a contraction mode  $q = \pi_k$  with  $1 < k < p$ , a permutation of the  
 377 inner and outer tensor dimensions with their respective indices  $\pi_1, \dots, \pi_{k-1}$  and

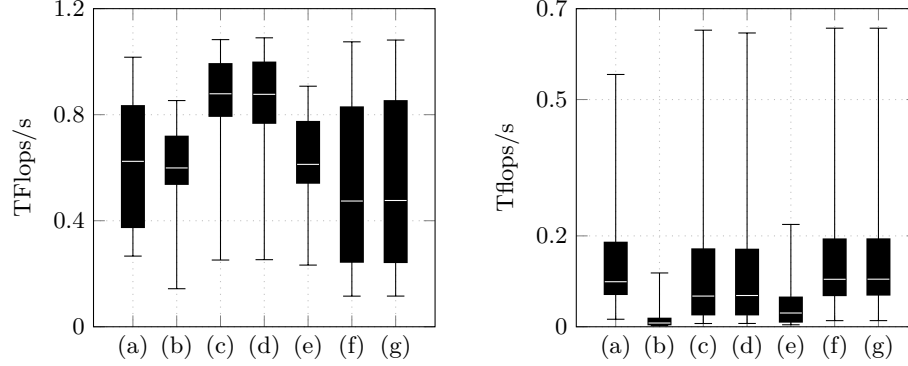


**Fig. 3.** Box plots visualizing performance statics in double-precision Tflops/s of a tensor-times-matrix algorithm for linear  $k$ -order tensor formats. The algorithm loops over single-threaded `gemm` with tensor slices with asymmetrically-shaped tensors on the left plot and with subtenors with symmetrically-shaped tensors on the right plot. Box plot number  $k$  denotes the utilized  $k$ -order storage.

378  $\pi_{k+1}, \dots, \pi_p$  does influence the runtime where the LB-PN version calls `GEMV` with  
 379 the values  $w_m$  and  $n_m$ . The same holds true for the outer layout tuple.

380 **Comparison with other Approaches** The following comparison includes  
 381 three state-of-the-art libraries that implement three different approaches. The  
 382 library `TCL` (v0.1.1) implements the (TTGT) approach with a high-perform tensor-  
 383 transpose library `HPTT` which is discussed in [17]. `TBLIS` (v1.0.0) implements  
 384 the `GETT` approach that is akin to `BLIS`'s algorithm design for matrix computa-  
 385 tions [12]. The tensor extension of `EIGEN` (v3.3.90) is used by the Tensorflow  
 386 framework and performs the tensor-vector multiplication in-place and in paral-  
 387 lel with contiguous memory access [1]. `TLIB` denotes our library that consists of  
 388 sequential and parallel versions of the tensor-vector multiplication. Numerical  
 389 results of `TLIB` have been verified with the ones of `TCL`, `TBLIS` and `EIGEN`.

390 Fig. ?? illustrates the average single-precision Gflops/s with asymmetrically-  
 391 and symmetrically-shaped tensors in the first-order storage format. The run-  
 392 time behavior of `TBLIS` and `EIGEN` with asymmetrically-shaped tensors is almost  
 393 constant for varying tensor sizes with a standard deviation ranging between 2%  
 394 and 13%. `TCL` shows a different behavior with 2 and 4 Gflops/s for any order  
 395  $p \geq 2$  peaking at  $p = 10$  and  $q = 2$ . The performance values however deviate  
 396 from the mean value up to 60%. Computing the arithmetic mean over the set  
 397 of contraction modes yields a standard deviation of less than 10% where the  
 398 performance increases with increasing order peaking at  $p = 10$ . `TBLIS` performs  
 399 best for larger contraction dimensions achieving up to 7 Gflops/s and slower run-  
 400 times with decreasing contraction dimensions. In case of symmetrically-shaped  
 401 tensors, `TBLIS` and `TCL` achieve up to 12 and 25 Gflops/s in single precision with  
 402 a standard deviation between 6% and 20%, respectively. `TCL` and `TBLIS` behave

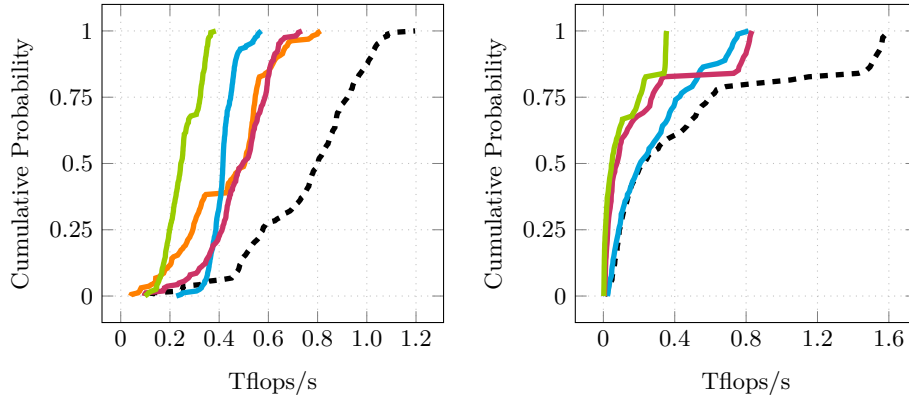


**Fig. 4.** Cumulative performance distributions of tensor-times-matrix algorithms in double-precision Tflops/s. Each distribution line belongs to a library: **tlib** (---), **tcl** (—), **tblis** (—), **libtorch** (—), **eigen** (—). Libraries have been tested with asymmetrically-shaped (left plot) and symmetrically-shaped tensors (right plot).

403 similarly and perform better with increasing contraction dimensions. **EIGEN** exe-  
 404 cutes faster with decreasing order and increasing contraction mode with at most  
 405 8 Gflops/s at  $p = 2$  and  $q \geq 2$ .

406 Fig. ?? illustrates relative performance maps of the same tensor-vector multi-  
 407 plication implementations. Comparing **TCL** performance, **TLIB-SB-PN** achieves an  
 408 average speedup of 6x and more than 8x for 42% of the test cases with asymmetri-  
 409 cally shaped tensors and executes on average 5x faster with symmetrically shaped  
 410 tensors. In comparison with **TBLIS**, **TLIB-SB-PN** computes the tensor-vector prod-  
 411 uct on average 4x and 3.5x faster for asymmetrically and symmetrically shaped  
 412 tensors, respectively.

## 413 7 Conclusion and Future Work

414 Based on the **LOG** approach, we have presented in-place and parallel tensor-vector  
 415 multiplication algorithms of **TLIB**. Using highly-optimized **DOT** and **GEMV** routines  
 416 of **OpenBLAS**, our proposed algorithms is designed for dense tensors with arbi-  
 417 trary order, dimensions and any non-hierarchical storage format. **TLIB**'s algo-  
 418 rithms either directly call **DOT**, **GEMV** or recursively perform parallel slice-vector  
 419 multiplications using **GEMV** with tensor slices and fibers.

420 Our findings show that loop-fusion improves the performance of **TLIB**'s par-  
 421 allel version on average by a factor of 5x achieving up to 34.8/15.5 Gflops/s in  
 422 single/double precision for asymmetrically shaped tensors. With symmetrically  
 423 shaped tensors resulting in small contraction dimensions, the results suggest that  
 424 higher-order slices with larger dimensions should be used. We have demonstrated  
 425 that the proposed algorithms compute the tensor-vector product on average 6.1x  
 426 and up to 12.6x faster than the **TTGT**-based implementation provided by **TCL**. In

comparison with TBLIS, TLIB achieves speedups on average of 4.0x and at most 10.4x. In summary, we have shown that a LOG-based tensor-vector multiplication implementation can outperform current implementations that use a TTGT and GETT approaches.

In the future, we intend to design and implement the tensor-matrix multiplication with the same requirements also supporting tensor transposition and subtensors. Moreover, we would like to provide an in-depth analysis of LOG-based implementations of tensor contractions with higher arithmetic intensity.

**Project and Source Code Availability** TLIB has evolved from the Google Summer of Code 2018 project for extending Boost’s uBLAS library with tensors. Project description and source code can be found at <https://github.com/bassoy/ttv>. The sequential tensor-vector multiplication of TLIB is part of uBLAS and in the official release of Boost v1.70.0.

**Acknowledgements** The author would like to thank Volker Schatz and Banu Sözüar for proofreading. He also thanks Michael Arens for his support.

## References

1. Abadi, M., Barham, P., Chen, J., Chen, Z., Davis, A., Dean, J., Devin, M., ..., Zheng, X.: Tensorflow: A system for large-scale machine learning. In: Proceedings of the 12th USENIX Conference on Operating Systems Design and Implementation. pp. 265–283. OSDI’16, USENIX Association, Berkeley, CA, USA (2016)
2. Bader, B.W., Kolda, T.G.: Algorithm 862: Matlab tensor classes for fast algorithm prototyping. ACM Trans. Math. Softw. **32**, 635–653 (December 2006)
3. Başsoy, C.: Design of a high-performance tensor-vector multiplication with blas. In: International Conference on Computational Science. pp. 32–45. Springer (2019)
4. Başsoy, C., Schatz, V.: Fast higher-order functions for tensor calculus with tensors and subtensors. In: International Conference on Computational Science. pp. 639–652. Springer (2018)
5. Golub, G.H., Van Loan, C.F.: Matrix Computations. JHU Press, 4 edn. (2013)
6. Goto, K., Geijn, R.A.v.d.: Anatomy of high-performance matrix multiplication. ACM Transactions on Mathematical Software (TOMS) **34**(3) (2008)
7. Karahan, E., Rojas-López, P.A., Bringas-Vega, M.L., Valdés-Hernández, P.A., Valdes-Sosa, P.A.: Tensor analysis and fusion of multimodal brain images. Proceedings of the IEEE **103**(9), 1531–1559 (2015)
8. Kolda, T.G., Bader, B.W.: Tensor decompositions and applications. SIAM review **51**(3), 455–500 (2009)
9. Lee, N., Cichocki, A.: Fundamental tensor operations for large-scale data analysis using tensor network formats. Multidimensional Systems and Signal Processing **29**(3), 921–960 (2018)
10. Li, J., Battaglini, C., Perros, I., Sun, J., Vuduc, R.: An input-adaptive and in-place approach to dense tensor-times-matrix multiply. In: High Performance Computing, Networking, Storage and Analysis, 2015 SC-International Conference for. pp. 1–12. IEEE (2015)

- 469 11. Lim, L.H.: Tensors and hypermatrices. In: Hogben, L. (ed.) Handbook of Linear  
470 Algebra. Chapman and Hall, 2 edn. (2017)
- 471 12. Matthews, D.A.: High-performance tensor contraction without transposition.  
472 SIAM Journal on Scientific Computing **40**(1), C1–C24 (2018)
- 473 13. Napoli, E.D., Fabregat-Traver, D., Quintana-Ortí, G., Bientinesi, P.: Towards an  
474 efficient use of the blas library for multilinear tensor contractions. Applied Math-  
475 ematics and Computation **235**, 454 – 468 (2014)
- 476 14. Papalexakis, E.E., Faloutsos, C., Sidiropoulos, N.D.: Tensors for data mining and  
477 data fusion: Models, applications, and scalable algorithms. ACM Transactions on  
478 Intelligent Systems and Technology (TIST) **8**(2), 16 (2017)
- 479 15. Shi, Y., Niranjana, U.N., Anandkumar, A., Cecka, C.: Tensor contractions with  
480 extended blas kernels on cpu and gpu. In: 2016 IEEE 23rd International Conference  
481 on High Performance Computing (HiPC). pp. 193–202 (Dec 2016)
- 482 16. Solomonik, E., Matthews, D., Hammond, J., Demmel, J.: Cyclops tensor frame-  
483 work: Reducing communication and eliminating load imbalance in massively par-  
484 allel contractions. In: Parallel & Distributed Processing (IPDPS), 2013 IEEE 27th  
485 International Symposium on. pp. 813–824. IEEE (2013)
- 486 17. Springer, P., Bientinesi, P.: Design of a high-performance gemm-like tensor–tensor  
487 multiplication. ACM Transactions on Mathematical Software (TOMS) **44**(3), 28  
488 (2018)